

High pressure Raman scattering of silicon nanowires

This article has been downloaded from IOPscience. Please scroll down to see the full text article.

2011 Nanotechnology 22 195707

(<http://iopscience.iop.org/0957-4484/22/19/195707>)

View [the table of contents for this issue](#), or go to the [journal homepage](#) for more

Download details:

IP Address: 129.169.177.88

The article was downloaded on 30/03/2011 at 12:17

Please note that [terms and conditions apply](#).

High pressure Raman scattering of silicon nanowires

Sevak Khachadorian¹, Konstantinos Papagelis^{2,3}, Harald Scheel¹, Alan Colli⁴, Andrea C Ferrari⁵ and Christian Thomsen¹

¹ Institut für Festkörperphysik, Technische Universität Berlin, 10623 Berlin, Germany

² Materials Science Department, University of Patras, 26504 Patras, Greece

³ Institute of Chemical Engineering and High Temperature Chemical Processes, Stadiou str. Platani, P. O. Box 1414, Patras 26504, Greece

⁴ Nokia Research Centre, 21 J J Thomson Avenue, Cambridge CB3 0FA, UK

⁵ Department of Engineering, University of Cambridge, Cambridge CB3 0FA, UK

E-mail: khachadorian@physik.tu-berlin.de

Received 4 October 2010, in final form 12 February 2011

Published 23 March 2011

Online at stacks.iop.org/Nano/22/195707

Abstract

We study the high pressure response, up to 8 GPa, of silicon nanowires (SiNWs) with ~ 15 nm diameter, by Raman spectroscopy. The first order Raman peak shows a superlinear trend, more pronounced compared to bulk Si. Combining transmission electron microscopy and Raman measurements we estimate the SiNWs' bulk modulus and the Grüneisen parameters. We detect an increase of Raman linewidth at ~ 4 GPa, and assign it to pressure induced activation of a decay process into LO and TA phonons. This pressure is smaller compared to the ~ 7 GPa reported for bulk Si. We do not observe evidence of phase transitions, such as discontinuities or change in the pressure slopes, in the investigated pressure range.

(Some figures in this article are in colour only in the electronic version)

1. Introduction

Materials with dimensions ranging from a few angstroms to several nanometers can be routinely synthesized by a number of techniques [1]. Owing to their confined size and high surface-to-volume ratio, these can show different mechanical, electronic and optical properties from those of bulk [1–5]. Nanostructured silicon is particularly interesting, because present-day information technology is still largely pinned on this widely available material. Silicon nanowires (SiNWs) have stimulated extensive efforts, ranging from the integration of optoelectronic devices into Si microelectronics [6–8] to large-area applications such as photovoltaics [9–11] and thermoelectrics [12, 13].

Raman spectroscopy has proven to be an effective and nondestructive characterization technique to understand the lattice dynamics of SiNWs [14–20]. Phonon frequencies and linewidths give valuable information about microscopic parameters such as bonding and structure as well as deviations from the crystalline counterpart [21–23]. The available data on SiNWs' mechanical properties show significant differences. Some report a Young and bulk modulus decrease with respect

to bulk Si, depending on diameter [24–27], while others claim an opposite trend [28, 29, 2].

Here, we perform Raman scattering experiments to investigate the influence of hydrostatic pressure on the longitudinal and transversal optical (LTO) optical phonon mode of SiNWs with a mean diameter of ~ 15 nm. We find a slightly more pronounced pressure dependence compared to bulk Si. In particular, the Raman linewidth shows a significant increase above a critical pressure (~ 4 GPa), which we assign to the activation of an additional decay channel into LO + TA phonons.

2. Experimental details

SiNWs are grown by vapor transport [20]. SiO powder is evaporated at $\sim 1400^\circ\text{C}$ in a horizontal tube furnace for 3 h. The Si vapor condenses at $\sim 900^\circ\text{C}$ on a quartz substrate. The average wire diameter is ~ 15 nm, consisting of an outer 2–3 nm SiO₂ shell and a crystalline Si core. During synthesis, Ar is allowed to flow (100 sccm) as carrier gas at pressures close to atmospheric (800–1000 mbar). In parallel with SiNW growth, reduction of the pressure enhances the formation of

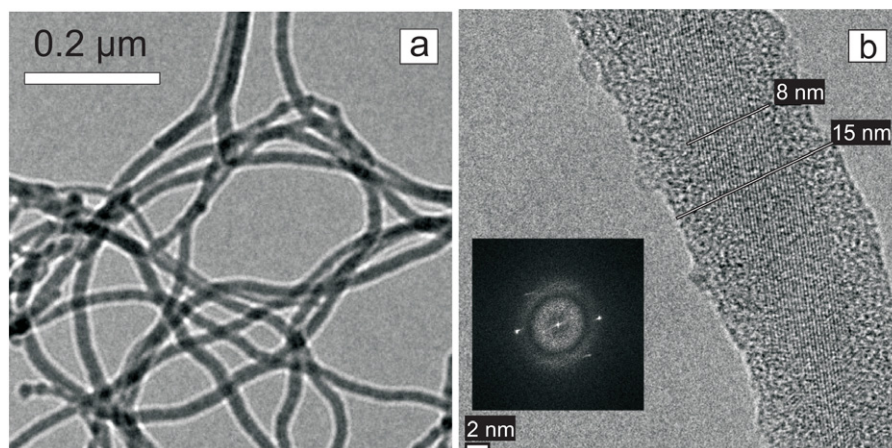


Figure 1. (a) Representative morphology of our SiNW sample. (b) Individual SiNW and (inset) its diffraction pattern.

Table 1. Lattice parameter, a , nearest-neighbor distance, d , and bulk moduli of SiNWs. For comparison the values for bulk Si are included.

Sample	a (Å)	$d^{-3.5}$ (Å)	K_0 (GPa)	Reference
SiNWs (15 nm)	5.57(5)	0.046(1)	—	This study
SiNWs (15 nm)	0.5437	0.0499	—	[34]
SiNWs (15 nm)	5.435	0.0500	—	[21]
SiNWs (70 nm)	5.423(2)	0.0504(1)	123(5)	[36]
SiNWs (22 nm)	5.448	0.0496	—	[35]
Bulk Si	5.43	0.05017	100(2)	[33]
Bulk Si	5.435	0.0500	99.9	[41]
Bulk Si	5.435	0.0500	94.8	[42]

Si–SiO₂ nanochains, i.e., filamentary nanostructures where crystalline Si spheres are connected by SiO₂ bridges of variable length [20, 30].

The initial characterization of the sample is performed with a 200 kV transmission electron microscope (TEM) (Tecnai G²20 from FEI). The macro-Raman setup consists of a Dilor-XY 800 spectrometer equipped with a triple monochromator and a charge coupled device (CCD) with $\lambda = 514.5$ nm excitation from an Ar⁺ laser, in back-scattering geometry, with 1.0 cm⁻¹ resolution. Pressure measurements are carried out with a Syassen–Holzapfel–diamond anvil cell [31] with a 4:1 methanol–ethanol mixture as pressure medium, to ensure good hydrostatic conditions at least up to 10 GPa. The ruby fluorescence [32] is used for pressure calibration. The spectra are fitted with Voigt functions after background subtraction.

3. Results and discussion

Figure 1(a) shows the SiNWs' morphology. They have a core diameter of ~ 8 nm and an amorphous SiO₂-coating of ~ 3.5 nm, as seen in figure 1(b). The inset of figure 1(b) plots the Fourier-transform of the crystallographic planes of an individual SiNW. This indicates that the crystallographic growth direction is unchanged along this SiNW. A change would be indicated by more reflections in the Fourier-transformed image. From the diffraction pattern, the lattice

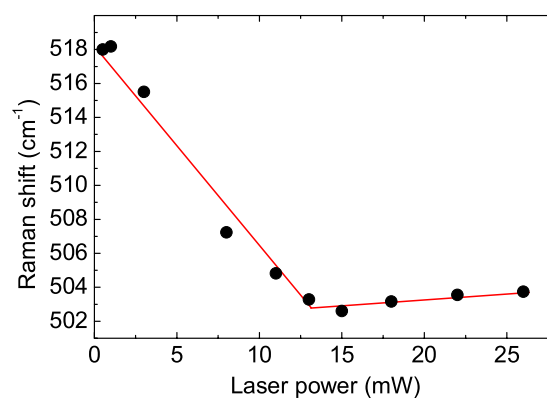


Figure 2. LTO frequency as a function of laser power, for 514.5 nm excitation. The line is a guide to the eye.

parameter (a) is determined to be 5.57 ± 0.05 Å. Figures 1(a) and (b) show a lattice parameter expansion of $\sim 2\%$, compared to bulk Si (5.43 Å [33]). This is consistent with previous x-ray diffraction (XRD) studies of SiNWs, where a larger lattice parameter compared to bulk Si was reported (0.1% [34], 0.4% [21], or 0.31% [35]). However, other TEM imaging work found a smaller one (0.14%) [36], table 1.

A high excitation power can increase the local temperature in SiNWs, causing a red shift and a broadening of the Raman peaks [14–16]. Therefore the laser power must be kept at a low level to avoid such local heating effects. This effect is negligible in bulk Si because of the better thermal conductivity of the bulk crystal [14, 37–40]. Thus, we first consider the possibility of thermal effects by studying the LTO mode as a function of excitation power, see figure 2. We detect a softening with increasing power at a rate of 1.27 cm⁻¹ mW⁻¹ up to 13 mW, followed by saturation. This softening is reversible. The extrapolated zero-power Raman peak position is 518.9 ± 0.6 cm⁻¹. The Raman red shift caused by overheating depends on the thermal anchoring of the SiNWs to the substrate [14] and the thermal conductivity of the surrounding gas [14, 15, 17]. These factors, together with the power density on the laser spot, which depends on the micro- or macro-experimental

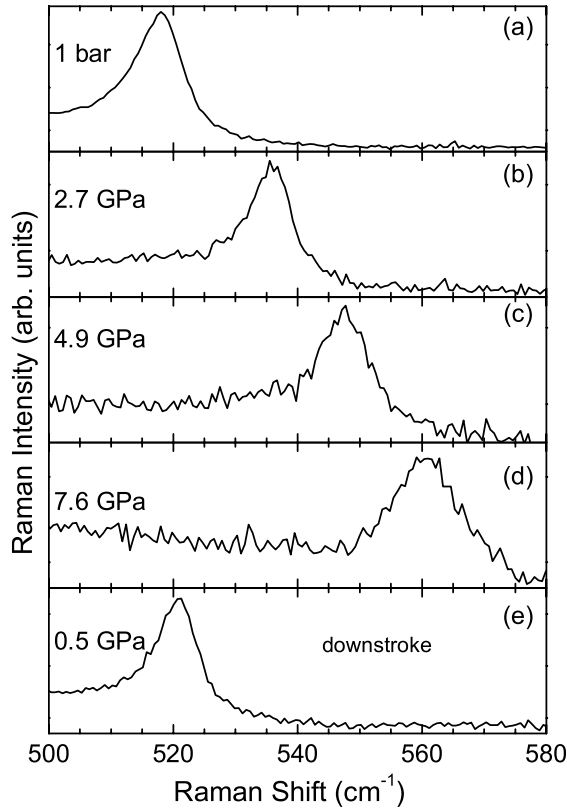


Figure 3. Raman spectra of SiNWs at various hydrostatic pressures, recorded ((a)–(d)) upon pressure increase, and (e) after pressure decrease, for 514.5 nm excitation.

setup, influence the value of the frequency versus power slope. This value was reported as $0.5 \text{ cm}^{-1} \text{ mW}^{-1}$ [15] and $1 \text{ cm}^{-1} \text{ mW}^{-1}$ [43, 17] for a macro-Raman setup, and $\sim 2.5 \text{ cm}^{-1} \text{ mW}^{-1}$ [44] for a micro-one. Furthermore, [17] reported a linear dependence of this slope with the inverse thermal conductivity of the medium surrounding the SiNWs. In our high pressure setup, the medium is a methanol–ethanol mixture with thermal conductivity (0.204 W mK^{-1} for methanol [45] and 0.168 W mK^{-1} for ethanol [46]) higher than air (0.024 W mK^{-1} [47]). Therefore, we conclude that the laser induced overheating in our high pressure Raman measurements performed for $\sim 1.5 \text{ mW}$ excitation power should be about ten times smaller than in air, and thus negligible.

Figure 3 plots the Raman spectra of SiNWs recorded for increasing pressures. This shows an upshift and broadening of the LTO Raman peak, with no change of lineshape. We assume the Raman signal collected from necklace shaped nanostructures to be negligible, due to their small concentration in our sample. Figure 4 plots the fitted pressure evolution of the LTO peak. We note that the effect of the compression and the decompression processes on the Raman spectra is reversible, as confirmed by the pressure dependence of the LTO peak full width at half maximum (FWHM) in figure 5. We fit the data in figure 4 with a quadratic function of pressure:

$$\omega(P) = 519.11(6) [\text{cm}^{-1}] + 6.11(4) [\text{cm}^{-2} \text{ GPa}^{-2}] \cdot P - 0.080(5) [\text{cm}^{-2} \text{ GPa}^{-2}] \cdot P^2. \quad (1)$$

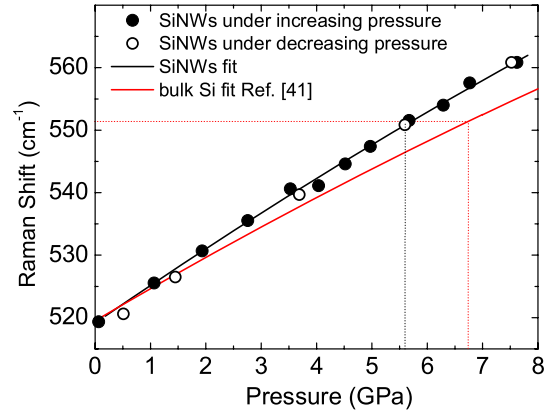


Figure 4. Pressure dependence of the LTO optical phonon in SiNWs. The black solid (open) circles denote data under increasing (decreasing) pressure. The red solid line corresponds to the pressure dependence of bulk Si from [41].

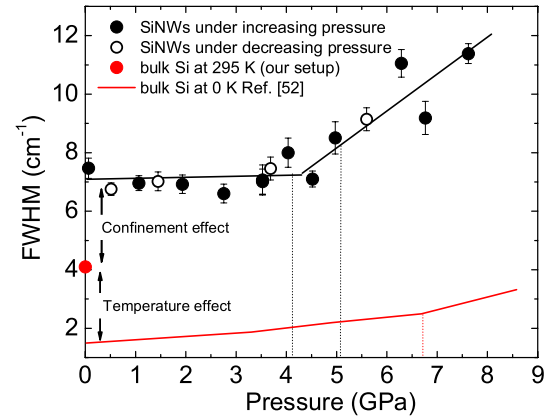


Figure 5. Pressure dependence of the LTO mode FWHM in SiNWs and bulk Si. The filled (open) circles refer to increasing (decreasing) pressure for SiNWs. The red solid line corresponds to the calculated trend for bulk Si at 0 K from [52]. The red solid circle is our measured FWHM of bulk Si at 295 K.

For comparison, figure 4 also plots the room temperature pressure dependence for bulk Si, taken from [41]. Quadratic terms in the pressure dependence of the Raman frequencies originate from the nonlinear relationship between the relative lattice compression Δa and the external pressure P [48]. The volume dependent change for a phonon of frequency ω is characterized by the Grüneisen parameter γ , defined as [49]

$$\gamma = -\frac{d \ln \omega}{d \ln V} = \frac{1}{\beta} \frac{\partial \ln \omega}{\partial P} = \left(\frac{K_0}{\omega} \right) \left(\frac{d\omega}{dP} \right) \quad (2)$$

where K_0 is the bulk modulus, β the isothermal volume compressibility and V the molar volume in $\text{cm}^3 \text{ mol}^{-1}$. Combining the fit parameters from equations (1) and (2), we get $\gamma/K_0 = (11.77 \pm 0.08) \times 10^{-3} \text{ GPa}^{-1}$ and $\gamma\beta = (10.1 \pm 0.2) \times 10^{-3} \text{ GPa}^{-1}$ for our SiNWs, as reported in table 2. The corresponding bulk Si values using the data in [41] are also shown in table 2. These are $\sim 17\%$ (10%) smaller than those for our SiNWs, respectively, suggesting that our SiNWs have a smaller bulk modulus than bulk Si.

Table 2. Phonon frequency at zero pressure, linear and quadratic pressure coefficients, γ/K_0 and $\gamma\beta$, for our SiNWs. The corresponding values for bulk Si are also included.

Sample	ω_0 (cm^{-1})	$\frac{d\omega}{dP}$ (GPa cm^{-1})	$-\frac{d^2\omega}{dP^2} \times 10^{-2}$ (GPa cm^{-2})	$\frac{\gamma}{K_0} \times 10^{-3}$ (GPa^{-1})	$\gamma\beta \times 10^{-3}$ (GPa^{-1})	Reference
SiNWs	519.11(6)	6.11(4)	8.0(5)	11.77(8)	10.2(2)	This study
Bulk Si	519.5(8)	5.2(3)	7.0(2)	10.0(6)	9.2(5)	[41]
Bulk Si	518.6	5.5	8.6	10.61	—	[42]

Table 3. Grüneisen parameter, γ , and isothermal volume compressibility, β , calculated using the estimated bulk modulus from equation (3). The corresponding values for bulk Si are also reported.

Sample	a (Å)	K_0 (GPa)	K_0 (equation(3)) (GPa)	γ	$\beta(\times 10^{-3})$ (GPa^{-1})	Reference
SiNWs	5.57(5)	—	90(3)	1.06(3)	9.6(4)	This study
Bulk Si	5.435	99.9	98.26	0.98(6)	9.4(9)	[41]
Bulk Si	5.435	94.8	98.26	1.00115	—	[42]

The calculation of γ and β requires the knowledge of the bulk modulus of the SiNWs (see equation (2)) [49]. In [50] a formula was suggested to determine the bulk modulus of diamond and zinc-blend semiconductors:

$$K_0 \text{ (GPa)} = c \times d \text{ (Å)}^{-3.5} \quad (3)$$

with K_0 the bulk modulus and d the nearest-neighbor distance. In [50] the proportionality constant c in equation (3) was reported to be $1971 \text{ GPa Å}^{3.5}$. Table 1 presents a literature survey of the experimental lattice parameters and bulk moduli of SiNWs and bulk Si. Combining these values and equation (3) we estimate an average $c \sim 1962 \text{ GPa Å}^{3.5}$.

The measured lattice parameter a for our SiNWs is $5.57 \pm 0.05 \text{ Å}$. The corresponding nearest-neighbor distance is $d = a \times \sqrt{3}/4 = 2.41 \pm 0.02 \text{ Å}$. Thus, the extracted bulk modulus using equation (3) is $90 \pm 3 \text{ GPa}$, which is $\sim 11\%$ smaller than that for bulk Si. This allows us to estimate $\gamma = 1.06 \pm 0.03$ and $\beta = (9.6 \pm 0.04) \times 10^{-3} \text{ GPa}^{-1}$ for our SiNWs, as reported in table 3. These results indicate a smaller bulk modulus, and thus a bigger compressibility for our SiNWs compared to bulk Si. We note that [36] reported an increased bulk modulus ($123 \pm 5 \text{ GPa}$) for SiNWs with $\sim 70 \text{ nm}$ diameter, as derived from high pressure synchrotron measurements. However, their lattice parameter was 5.423 Å , i.e. $\sim 0.13\%$ smaller than for bulk Si. Others reported a larger lattice parameter, and consequently a smaller bulk modulus [34, 21], see table 1.

We now take a closer look at the pressure dependence of the Raman linewidths. The observed lineshape corresponds to the convolution of a Lorentzian peak with the Gaussian instrumental profile, i.e. a Voigt profile [51]. To determine the linewidth of the Lorentzian component, we fit the experimental data with a Voigt profile having a fixed width of 2.6 cm^{-1} for the Gaussian component, as determined by the FWHM of a neon line spectrum. The pressure dependence of the LTO peak position and FWHM for our SiNWs and bulk Si are shown in figure 5. The filled (open) circles refer to pressure increase (decrease). The trends are fully reversible. Figure 5 also plots the pressure dependence of the bulk Si FWHM at 0 K (red solid line) calculated in [52]. The FWHM of our

SiNWs at ambient pressure is $\sim 7 \text{ cm}^{-1}$, i.e. $\sim 6 \text{ cm}^{-1}$ larger than the theoretical results for bulk Si (1.4 cm^{-1} at 0 K). Figure 5 also shows the FWHM of bulk Si measured in ambient conditions (red solid circle) with our Raman setup. According to [53] the bulk Si Raman FWHM changes from 1.4 cm^{-1} (theoretical value) to 4 cm^{-1} for a temperature increase from 0 to 295 K. We conclude that the 2.5 cm^{-1} residual FWHM difference between our SiNWs and the calculated FWHM is related to the measurement temperature (increasing the FWHM from that calculated at 0 K to that corresponding to ambient temperature). The remainder of this difference (from 4 to 7 cm^{-1}) can be assigned to phonon confinement, as for [14], where a confinement related broadening of $\sim 2.5 \text{ cm}^{-1}$ was reported for SiNWs with an 8 nm diameter.

The FWHM increase for pressures up to 7 GPa in bulk Si was assigned to the decay of LTO into LA + TA phonons [52]. According to energy and momentum conservation the LTO phonon can decay into two phonons with total energy corresponding to the primary LTO phonon and opposite momentum. The bulk Si FWHM shows a remarkable increase above a critical pressure of $\sim 7 \text{ GPa}$ (see figure 5) [52]. When the pressure increases a new channel (decay of the LTO phonon into LO + TA phonons) related to wavevector regions around the high symmetry K and L points of the Brillouin zone begins to contribute [52]. The final states of this decay channel are TA and LO modes, forbidden at zero pressure, but allowed due to pressure induced effects. In the case of our SiNWs, this new decay channel becomes active at $\sim 4 \text{ GPa}$, causing the change in slope of FWHM as a function of pressure (P) in figure 5. As the crystal is restricted in one or more dimensions, the phonon scattering will not be limited to the center of the Brillouin zone, and the phonon dispersions near the zone center must also be considered. As a result, these symmetry-forbidden modes will be observed, in addition to shift and broadening of the Raman-allowed optical phonon. The larger pressure coefficient for our SiNWs also indicates a reduced onset of the additional decay channel. For a rough estimate, we compare the bulk Si Raman position at 7 GPa (551 cm^{-1}) with the pressure needed to generate the same Raman shift in SiNWs ($\sim 5.5 \text{ GPa}$). The

difference (1.5 GPa) is of the same magnitude as the decreased decay onset.

4. Conclusions

We studied by Raman spectroscopy ~ 15 nm diameter SiNWs as a function of pressure, up to 8 GPa. We detected a more pronounced pressure dependence compared to bulk Si. Using a phenomenological formula and the lattice parameter extracted from TEM measurements, we estimated the bulk modulus and the Grüneisen parameter of our SiNWs. We also found a remarkable FWHM increase at ~ 4 GPa, which we assigned to the pressure induced activation of a decay process of the zone center LTO optical phonon into LO and TA phonons. We did not detect any evidence of phase transition in the investigated pressure region, nor hysteresis during the decrease of pressure.

Acknowledgments

The authors thank D Berger and S Selve from Technische Universität Berlin ZELMI center for their support in conducting the TEM measurements. ACF acknowledges funding from EU grant NANOPOTS, and a Royal Society Wolfson Research Merit Award, from the Cambridge Integrated Knowledge Centre in Advanced Manufacturing Technologies for Photonics and Electronics and the Nokia Research Centre Cambridge.

References

- [1] Schmidt V, Wittemann J V and Gosele U 2010 *Chem. Rev.* **110** 361
- [2] Wang Z and Coffer L J 2004 *Phys. Chem. B* **108** 2497
- [3] Wang Z and Coffer L J 2002 *Nano Lett.* **2** 1303
- [4] Zhao X, Wei C M, Yang L and Chou M Y 2004 *Phys. Rev. Lett.* **92** 236805
- [5] Ma D D D, Lee C S, Au F C K, Tong S Y and Lee S T 2003 *Science* **299** 1874
- [6] Lee S T, Wang N and Lee C S 2000 *Mater. Sci. Eng. A* **286** 16
- [7] Bhattacharya S, Banerjee D, Adu K W, Samui S and Bhattacharyya S 2004 *Appl. Phys. Lett.* **85** 2008
- [8] Servati P, Colli A, Hofmann S, Fu Y Q, Beecher P, Durrani Z A K, Ferrari A C, Flewitt A J, Robertson J and Milne W I 2007 *Physica E* **38** 64
- [9] Sivakov V, Andrä G, Gawlik A, Berger A, Plentz J, Falk F and Christiansen S H 2009 *Nano Lett.* **9** 1549
- [10] Stelzner T, Pietsch M, Andrä G, Falk F, Ose E and Christiansen S 2008 *Nanotechnology* **19** 295203
- [11] Jeon M and Kamisako K 2009 *Mater. Lett.* **63** 777
- [12] Hicks L D and Dresselhaus M S 1993 *Phys. Rev. B* **47** 16631
- [13] Zhang Y, Christofferson J, Shakouri A, Deyu L, Majumdar A, Yiyang W, Rong F and Peidong Y 2006 *IEEE Trans. Nanotechnol.* **5** 67
- [14] Piscanec S, Cantoro M, Ferrari A C, Zapien J A, Lifshitz Y, Lee S T, Hofmann S and Robertson J 2003 *Phys. Rev. B* **68** 241312
- [15] Khachadorian S, Scheel H, Cantoro M, Colli A, Ferrari A C and Thomsen C 2009 *Phys. Status Solidi b* **246** 2809
- [16] Scheel H, Khachadorian S, Cantoro M, Colli A, Ferrari A C and Thomsen C 2008 *Phys. Status Solidi b* **245** 2090
- [17] Scheel H, Reich S, Ferrari A C, Cantoro M, Colli A and Thomsen C 2006 *Appl. Phys. Lett.* **88** 233114
- [18] Colli A, Fasoli A, Ronning C, Pisana S, Piscanec S and Ferrari A C 2008 *Nano Lett.* **8** 2188
- [19] Hofmann S, Ducati C, Neill R J, Piscanec S, Ferrari A C, Geng J, Dunin-Borkowski R E and Robertson J 2003 *J. Appl. Phys.* **94** 6005
- [20] Colli A *et al* 2007 *J. Appl. Phys.* **102** 034302
- [21] Wang R P, Zhou G W, Liu Y L, Pan S H, Zhang H Z, Yu D P and Zhang Z 2000 *Phys. Rev. B* **61** 16827
- [22] Kohnoa H, Iwasaki T, Mita Y and Takeda S 2002 *J. Appl. Phys.* **91** 3232
- [23] Qi J, White J M, Belcher A M and Masumoto Y 2003 *Chem. Phys. Lett.* **372** 763
- [24] Han X, Zheng K, Zhang X, Zhang Z and Wang Z 2007 *Adv. Mater. B* **19** 2112
- [25] Li X, Ono T, Wang Y and Esashi M 2003 *Appl. Phys. Lett.* **83** 3081
- [26] Kizuka T, Takatani Y, Asaka K and Yoshizaki R 2005 *Phys. Rev. B* **72** 035333
- [27] Tabib-Azar M, Nassirou M, Wang R, Sharma S, Kamins T I, Islamand M S and Williams R S 2005 *Appl. Phys. Lett.* **87** 113102
- [28] Heidelberg A, Ngo L T, Wu B, Phillips M A, Sharma S, Kamins T I, Sader J I and Boland J J 2006 *Nano Lett.* **6** 1101
- [29] Gordon J M, Baron T, Dhalluin F, Gentile P and Ferret P 2009 *Nano Lett.* **9** 525
- [30] Rafiq M A, Durrani Z A K, Mizuta H, Colli A, Servati P, Ferrari A C, Milne W I and Oda S 2008 *J. Appl. Phys.* **103** 053705
- [31] Huber G, Syassen K and Holzapfel W B 1977 *Phys. Rev. B* **15** 5123
- [32] Forman R A, Piermarini G J, Barnett J D and Block S 1972 *Science* **176** 248
- [33] McMahon M I, Nelmes R J, Wright N G and Allan D R 1994 *Phys. Rev. B* **50** 739
- [34] Yu D P *et al* 1998 *Appl. Phys. Lett.* **72** 3458
- [35] Su Z, Sha J, Pan G, Liu J, Yang D, Dickinson C and Zhou W 2006 *J. Phys. Chem. B* **110** 1229
- [36] Wang Y, Zhang J, Wu J, Coffer J L, Lin Zh, Sinogeikin S V, Yang W and Zhao Y 2008 *Nano Lett.* **8** 2891
- [37] Li D, Wu Y, Kim P, Shi L, Yang P D and Majumdar A 2006 *Appl. Phys. Lett.* **83** 2934
- [38] Mingo N 2003 *Phys. Rev. B* **68** 113308
- [39] Ponomareva I, Srivastava D and Menon M 2007 *Nano Lett.* **7** 1155
- [40] Boukai A I, Bunimovich Y, Tahir-Kheli J, Yu J K, Goddard W A and Heath J R 2008 *Nature* **451** 168
- [41] Weinstein B A and Piermarini G P 1975 *Phys. Rev. B* **12** 1172
- [42] Mernagh T P and Liu L G 1991 *J. Phys. Chem. Solids* **52** 507
- [43] Adu K W, Gutiérrez H R, Kim U J and Eklund P C 2006 *Phys. Rev. B* **73** 155333
- [44] Gupta R, Xiong Q, Adu C K, Kim U J and Eklund P C 2003 *Nano Lett.* **3** 627
- [45] Assael M J, Charitidou E and Nieto de Castro C A 1988 *Int. J. Thermophys.* **9** 813
- [46] Gray D E 1972 *American Institute of Physics Handbook* (New York: McGraw-Hill)
- [47] Young H D 1992 *University Physics* 7th edn (Reading, MA: Addison-Wesley)
- [48] Trommer R, Müller H, Cardona M and Vogel P 1980 *Phys. Rev. B* **21** 4869
- [49] Blackman M, Daniels W B, Cardona M and Güntherodt G (ed) 1984 *Light Scattering in Solids* vol IV (Berlin: Springer)
- [50] Cohen M L 1985 *Phys. Rev. B* **32** 7988
- [51] Posener D W 1959 *Aust. J. Phys.* **12** 184
- [52] Debernardi A, Baroni S and Molinari E 1995 *Phys. Rev. Lett.* **75** 1819
- [53] Balkanski M, Wallis M and Haro E 1983 *Phys. Rev. B* **28** 1928